RESEARCH ARTICLE

Editorial Process: Submission:09/18/2025 Acceptance:05/01/2026 Published:05/19/2026

Role of Cyanidin 3-glucoside Extract in the Induction of Cytotoxicity and Apoptosis in a Rat Bladder Cancer Cell Line

Haider Ammar Alubaidy[1], Ali Hamid Al-Bdeery[1], Esraa Abdul-Adel[2], Sarab A. Juda[3], Taghreed Hamed Abd_alameer[4], Majid Sakhi Jabir[5]*

Abstract

Objective: This study focused on organisms that produce natural bioactive compounds that are environmentally friendly alternatives to chemical treatments. These compounds include flavonoids derived from marine algae, including anthocyanins. Cyanidin-3-glucoside (C3G) is a natural pigment-protein complex capable of inhibiting or eradicating the proliferation of malignant cells, both in vivo and in vitro. **Methods:** This includes the AY-27 rat (BC) bladder cancer cell line. Its potential effects on inhibiting the production of isolated rat bladder tumor cells and activating cellular pathways were studied, including cytotoxicity, apoptosis, the *p53* pathway, mitochondrial wall loss pathway, and partial fusion. **Result:** The present study documented a peak mortality rate of 84.43% in the toxicity pathway on the maximum dose of 100 µg/ml of C3G. The minimum mortality rate of 9.45% was recorded at the maximum C3G concentration of 6.25 µg/ml. In the apoptotic process, dead cells were evaluated for DNA damage. C3G promotes mitochondrial failure in AY-27 cells via the mitochondrial pathway, leading to a reduction in mitochondrial membrane potential compared to untreated AY-27 cells. **Conclusion:** The study's findings showed that C3G increased *p53* gene expression in AY-27 cells during the *p53* pathway. The data in the tables and figures reveal that increasing the dose or concentration of C3G over time has a lethal effect on bladder cancer cells. The results indicate that C3G promotes localized apoptosis, thereby inhibiting and slowing down the progression of bladder cancer. These findings suggest that C3G could be an active natural treatment for BC in rats, with potential for further development by international pharmaceutical companies.

Keywords: cyanidin-3-glucoside- algal compounds- cytotoxicity- Rat Bladder Cancer- Apoptosis

Asian Pac J Cancer Prev, **27 (5)**, 1795-1804

Introduction

Recent studies have indicated that cancer includes a group of disorders characterised by uncontrolled cellular proliferation and the dissemination of atypical cells throughout the organism. Research has concentrated on creating novel therapeutic approaches to increase life expectancy and lower cancer mortality [1-3]. Cancer is still one of the biggest threats to global health is a significant cause of mortality globally, resulting in roughly ten million fatalities in 2020, and has adverse consequences [4, 5]. In recent years, biochemical molecules have surfaced as novel, eco-friendly anticancer medicines and viable alternatives to chemotherapy. Due to the worsening crisis of chemically synthesized treatments and medicines, the world's interest in these compounds from natural sources has increased. Marine organisms, such as brown algae, are at the forefront of these sources, offering a promising source of pharmaceutical compounds, in addition to plant sources. These natural compounds from algae, including brown algae Sargassum subrepandum, are rich in secondary metabolites anthocyanins (C3G and CCy3G), plants [1, 6], Flavonoids (including anthocyanins), sugars, lipids, polyphenols, and peptides with distinctive biological activity [7]. Recent studies have shown that bioactive compounds extracted from algal organisms have important therapeutic roles in preventing and inhibiting cancerous tumors [8].

Traditional and folk medicine have made use of natural items for therapeutic purposes. For instance, taxol and flavonoids like anthocyanidin and the well-known colchicine are among the numerous anticancer medications that have been employed in cancer chemotherapy that come from natural sources [9, 10]. Anthocyanins are among the more than 10,000 secondary metabolites that make up the families of polyphenolic chemicals known as flavonoids. Anthocyanidins are one of their aglycone forms. The quantity and location of hydroxyl and methoxyl substituents in their structure determine which classifications they fall under. Algae, such as seaweed and the plant Laminaria japonica, contain them [11-15]. The six major classes of natural anthocyanins that have

*[1]College of Science, Al Qadisiyah University, Iraq. [2]College of Environmental Sciences, Al-Qasim Green University, Iraq. [3]College of Science, University of Babylon, Iraq. [4]Al-Qadisiyah Education Directorate, Ministry of Education, Iraq. [5]College of Applied Sciences, University of Technology, Iraq. *For Correspondence: 100131@uotechnology.edu.iq*

emerged in recent years have important protective, health and industrial functions. They are cyanidin, delphinidin, betonidin, peonydin, pelargonin and malvidin, and they belong to the polyphenol class. The most significant of them is cyanidin-3-glucoside (C3G), a naturally occurring protein pigment found in various organisms and one of the most prevalent anthocyanins. Because of the hydroxyl group on the ring, C3G has potent antioxidant and anticancer properties. Vanillic acids (VA), ferric acid (FA), with protocatechuic acid (PCA), phloglucinaldehyde (PGA), and other C3G metabolites (C3G-Ms) and their derivatives are the main active bioactive metabolites of C3G, due to their anticancer properties, including those against bladder cancer, antioxidant and free radical scavenging, antibacterial and antifungal properties, and their potential applications in strategies to combat and treat diseases such as diabetes and atherosclerosis, among others. Therefore, this study recommended the inclusion of algae extracts or powder as a natural alternative to synthetic treatments or their use in pharmaceutical formulations and inflammation [1]. According to the amount and position of hydroxyl and methoxyl groups replaced in its structure, C3G has been classified into several kinds [14, 15].

Anthocyanin pigments contain 2 aromatic rings with 6 carbon atoms linked by a 3-c- h- ring. The 1ST ring (A) contains two hydroxyl groups and three double bonds, the 2nd ring (C) ring (C) contains one oxygen atom and two double bonds, and the third ring (B) contains one hydroxyl group, Tri- dual links, and two side functional groups. Anthocyanin pigments are the chemical compounds' R groups [16], as they are molecules that seek stability and non-degradation in the environment, and are characterized by their purple color, which gives the algae its name and color [1,17]. The stability of the structural forms of anthocyanins is attributed to their common pigmentation [18]. The anticancer and antioxidant activity of algal compounds, including anthocyanins, occurs due to molecular associations with other organic molecules, such as receptor proteins on the surface of cancer cells, which are often described as cofactors [19-23]. Owing to there high possible as antitumor bosses, these compounds have the potential to be considered as anticancer agents, as they inhibit the proliferation of tumor cells by stimulating the engineered cell death pathway and stopping the formation of blood containers, thus contributing to reducing the spread of cancer [13]. This is achieved through two important mechanisms: single-electron transport (SET) and hydrogen-atom transport (HAT). Their structure also enables them to exhibit anti-cancer properties and eliminate free radicals. Both processes reduce oxidative damage caused by primary free radicals by converting anthocyanins into a more stable free radical [24]. Through several pathways, anthocyanins also donate to cancer cell demise, plummeting the inflammatory response (COX inhibition), inhibiting the production of ROS, regulating cytokines that cause inflammation (TNF-α, IL-1β, and IL-6), inhibiting cell apoptosis through the Bcl-2/Bax ratio, and modulating the NF-B, AMPK, and MAPK pathways of signaling. Encouraging cell proliferation through the PI3K/Akt signaling pathway and decreasing enzymes that facilitate digestion, including α-amylase and α-glucosidase [25]. This study sought to examine the anticancer efficacy of the natural chemical cyanidin-3-glucoside (C3G) ،extracted from algae, on the AY-27 cancer cell line, through molecular and immunological pathways. It also aimed to explore its potential as a natural alternative to chemotherapy in killing bladder cancer cells. It also aimed to enhance our understanding To realise the potential benefits of algae's functional components, cellular and molecular pathways must be established., including cytotoxicity, apoptosis, and loss of mitochondrial wall capacity, were identified in C3G-induced cancer cell differentiation.

Materials and Methods

Preparation of Cyanidin-3-glucoside compound

The standard compound used is cyanidin-3-glucoside (C3G), an algae and plant extract manufactured by the same company and imported from the USA (Colorado Springs) by BIO TEST. It is packaged in a container with several purple capsules and boasts 97% purity.

preservation of cell cultures

The AY-27 cancerous bladder cell line was cultivated in RPMI-1640 media augmented with as much as ten percent fetal bovine serum, as well as penicillin up to 100 units/ml, and streptomycin up to 100 micrograms/ml. Using trypsin-EDTA, the cells were transfected and then re-cultured every two weeks at 80% of the cell density. The cells were then hatched at 37°C [26, 27].

Cytotoxicity Assay

The MTT test was used to assess the toxic to cells effect of C3G using 96-well plates [28, 29]. Cells were seeded at a thickness of 1×10^4 cells in each well. After 24 hours, or when a continuous single layer was reached, the AY-27 BC cellular lineage was treated with the natural compound C3G. Cell viability was evaluated at 24,48, and 72 hours after the C3G treatment by aspirating the medium. Subsequently, 100 µL of a 2 mg/ml solution of MTT was introduced, and the tumour cells were allowed to develop for a total of 2.5 hours at 37°C. Residual crystals in the wells post-MTT removal were solubilised by the addition of 130 µL of DMSO (dimethyl sulphuric sulfoxide) and thereafter agitated for fifteen minutes at 37°C with constant agitation [30]. We used a microplate reader to measure the absorbance at a wavelength of 492 nm. The exam was done three times. The cell growth suppression rate (cytotoxicity ratio) was then determined using the following equation [31, 32]:- Inhibition rate (%) = [(A − B) / A] × 100. The letter A stands for the ophthalmic density of the controlled sample. The letter B, on the other hand, stands for the samples' optical density [33]. Cancer cells were cultured in 24-well microplatelets with a density of 1×10^5 cells/ml to monitor cell morphological changes using an inverted microscope. The plates were kept at 37 degrees Celsius for twenty-four hours. Subsequently, the cancer cells were exposed to the natural compound C3G for 24 hours. After the exposure period, the microplatelets were stained with crystal violet and incubated for 10–15

minutes at 37°C [6]. The stain was then thoroughly rinsed with faucet water until complete removal was observed. The cells were then examined at 40x magnification and photographed with an electronic camera connected to the microscope [34].

Acridine Orange–Ethidium Bromide Staining

The AO/EtBr stain assay was used to assess the rate of chemically induced programmed death of AY-27 bladder cancer cells (Sigma-Aldrich, USA). After 24 hours of culture of AY-27 cancer cells in 24-well plates, the cancer cells were treated with the natural bio-compound C3G. The plates were then kept warm for another 20 h, and the cells were washed in twice as much phosphate-diluted saline. Then, 50 µL of the two fluorescent dyes was added to the wells for 2 minutes in equal amounts to the cells, and the cells were finally examined using a fluorescence microscope [35, 36].

Evaluation of Intracellular Reactive Oxygen Species Production

In C3G-treated and untreated AY-27 cancer cells, ROS generation was assessed employing a fluorescent pigment 2,7, DCFH-DA. Suspended droplets of AY-27 cells were treated with 10 µM DCFH-DA at room temperature in the dark for 45 minutes. During this time, the dye penetrated the cells and reacted within them with the ROS to produce the fluorescent compound dichlorofluorescein (DCF). The stained cells were placed on a clean microscope slide after incubation and then examined under a fluorescence microscope. Fluorescence images were then taken to visualize and assess ROS generation within the AY-27 cancer cells.

Apoptosis Detection by Flow Cytometry

To differentiate between apoptotic and necrotic cells, We employed the annexed V-Fluorescein Isothiocyanate (FITC) cell death identify kit (Abcam, Cambridge Science Park, Cambridge, UK) along with two-channel flow cytometry. After 24 hours of exposure to the natural bioactive compound C3G, AY-27 cancer cells were collected using trypsin. The cells were rinsed twice with cold saline solution with phosphate buffering (PBS), pH 7.2. The samples were subsequently treated at room temp in a dark place with a stain solution comprising Annexin V-FITC and PI, or Propidium iodide, at a concentration of 1 µg/ml for 45 minutes. The specimens were subsequently examined via flow cytometry. Using channels FL1 and FL2, we were able to see fluorescence signals for FITC and PI, respectively. Excitation and emission at 488 and 530 nm. PI: 535/617 nm. After that, ACEA Novo Express software and a spring assay (ACEA Biosciences, San Diego, CA, USA) were used to find out how many FITC and/or PI-positive cells there were.

Measurement of p53 Levels by Flow Cytometry Assay

To assess the stages of *p53* protein activation, the *p53* fluorescence stain kit (Thermos Fisher Scientific, USA) was used. The AY-27 cancer cell line (2×10^6 cells/ml) was cultured in 5 ml of middle for 24 hours at 37°C. The cultured Then, cells were treated with the natural biocompatible compound C3G for an additional 24 hours. After cultivation, the cured cells were collected and washed double with cold PBS at a 1× concentration. The sediment was then collected and cultured in growth medium, with the cell thickness adjusted to 1 million cells per milliliter. Before and after incubation at 37°C for 60 minutes. The cells obtained using this method were then incubated with FITC Mouse Anti-*p53* Antibody. After the period of incubation, the cells were subjected to two washes with a washing solutions (0.5 ml), thereafter transferred to flow cytometry tubes, and analyzed using this technique. The data were analyzed by BD Accurate C6 software.

Mitochondrial Membrane Potential Assay

To evaluate the effect of the natural compound C3G on the mitochondrial activity of AY-27 cancer cells, the Rhodamine (Rh123) fluorescent dye was utilized to assess the voltage across the mitochondrial membrane ($\Delta\Psi m$) before and during treatment with C3G. Cell lines were treated with C3G 24 h, after being cultured Inside plates with 96 wells. The cells were then stained with Rh123 at a concentrate of 5 µM at 37°C for 2 hours. Cells were subsequently separated with 0.2 milliliter's of Five% trypsin-EDTA solution and then centrifugation for 5 minutes at three hundred grammes. They were resuspended in FACS buffer (1-2% BSA in 1X PBS) and analyzed using flow cytometry, with the creation of graphs.

Molecular docking approach

The rat bladder cancer cell line serves as a crucial model for investigating the effects of natural compounds and their role in mitigating cellular damage associated with oxidative stress. Through laboratory studies, this cell line acts as a valued tool for understanding the interactions between these combinations and the cellular mechanisms that lead to cancer development. These compounds play a crucial role in reducing the impact of radicals that are free, which contribute to tumor progression, thereby enhancing the understanding of how they can be utilized in future therapeutic approaches. Molecular docking was employed to assess ligand interactions with the (Rat Bladder) Receptor (PDB ID: 5IRZ), giving binding scores that show how stable the complex is. The Protein Data Bank's main page (https://www.rcsb.org/structure/5IRZ) had the crystal structure on it. With an accuracy of 3.03 angstroms, the crystal structure is considered to be of good excellence for investigations of molecular docking. Two criteria are considered ideal for validating molecular docking outcomes: an RMSD (root-mean-square deviation) of 2 angstroms or less and an energy of -7 kcal/mol or less. Utilizing the Molecular Operational Environment (also known as MOE) software (MOE, 2022), the optimized molecules (the natural bioactive compound cyanidin 3-glucoside extracted from algae) were inserted into the receptor's active location. The docking and evaluation calculations were also carried out in the MOE program after the preparation of the receptor protein. To promote the establishment of possible hydrogen bonds between the target and the ligand while retaining water molecules in the active site, the missing bonds in the protein structure

were corrected, and the protein was proteolyzed after its structure was damaged during X-ray diffraction. Using the Energy Optimization-Assisted Model Building (AMBER 10), the protein structure was further optimized with the Extended Hooke's Theory (EHT) force field.

Statistical Analysis

To calculate the experimental information, we employed the Tukey's p-hoc test and the one-way ANOVA method. With a matched control group, the tests were done three times [37]. Data are presented as mean ± standard deviation. Linear regression was used to determine the IC50. OriginPro 2023 and GraphPad Prism version 7.0 were utilized for data analysis, with a significance level of $p < 0.05$. 95% confidence intervals and p-values were calculated for each analysis [38].

Results

The naturally occurring compound cyanidin-3-glucoside (C3G) induces cytotoxicity in AY-27 cells.

The findings of this investigation are presented in Figure 1 and Table 1, demonstrating the effect of the natural bioactive compound cyanidin-3-glucoside, extracted from algae, on AY-27 mouse bladder cancer cells. This was achieved by measuring its ability to induce harmful effects on AY-27 cells through the evaluation of C3G's antiproliferative efficacy. The bioactive compound C3G induced several significant morphological changes in AY-27 tumor cells after treatment, as illustrated in Figure 2. The study demonstrated a peak cytotoxicity rate of 84.43% with the use of the C3G compound at 100 µg/ml, while the lowest rate of 9.45% was recorded with the use of C3G at an amount of 6.25 microgrammes per millilitre.

Apoptosis pathway

Cyanidin-3-glucoside induce AY-27 cell death

The findings in the present investigation As illustrated in Figure 3, at an average concentration of 25 µg/ml, the study recorded a cell death rate of 44.56% (IC50, the halogenated concentration for half the cells)، showed the possibility of stimulating programmed cell death in AY-27 bladder cancer cells by the natural protein compound C3G. Cell growth slowdown often involves alterations in key signaling pathways due to changes in gene expression caused by activation of apoptosis pathways. Additionally, We used dual staining with acridine orange and ethidium bromide, which was performed to examine the morphology of cell nuclei treated with the natural compound, and based on DNA damage, dead cells were identified. This study also evaluated the activity of the C3G protein. To observe various necrotic changes in the cell nuclei, dual staining with AO-EB was used. Non-dead cells appeared green, while dead After being stained with AO-EtBr, the cells looked orange or red.

as The results indicated, as illustrated in Figure 4, a reduction in cancer cell viability that was directly proportional to the C3G concentration across five distinct levels (6.25, 12.5, 25, 50, and 100 µg/ml), with an IC_{50}

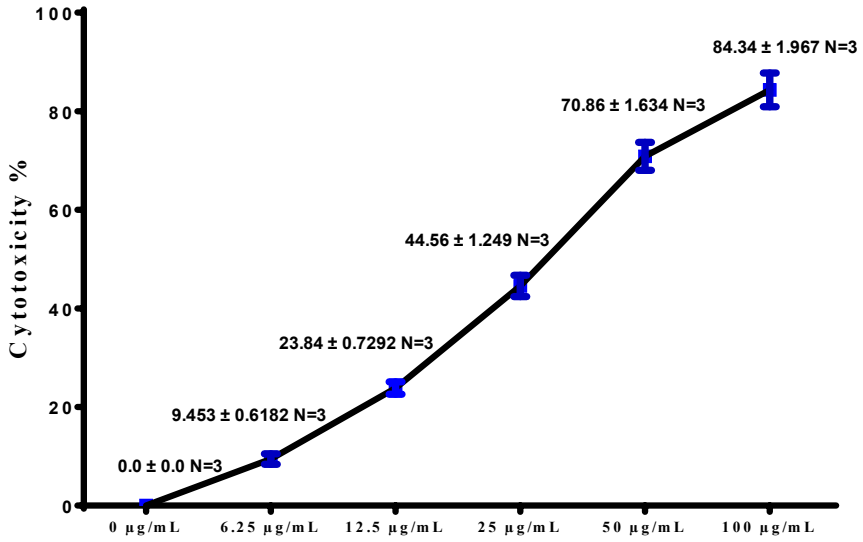

Figure 1. Cytotoxicity Effect of C3G in AY-27 cells. IC_{50} =25.08 µg\ml

Table 1. Cytotoxic Effect of C3G on AY-27 Cells

Cell Line AY-27	Concentration of Cyanidin-3-glucoside µg\ml					
Cytotoxicity %	0	6.25	12.5	25	50	100
Mean	0	9.45	23.84	44.56	70.86	84.43
SD	0	0.61	0.72	1.24	1.63	1.96
N	3	3	3	3	3	3

value of 25.08 µg/ml. Exposure to these doses resulted in a substantial elevation of ROS generation.

Cyanidin-3-glucoside causes mitochondrial dysfunction in AY-27 cells

In the results of this research in Figure 6, we measured metal matrix enzymes using flow cytometry in accordance with the manufacturer's specifications. Since the most important indicator of programmed cell death is a decrease in mitochondrial membrane potential, we employed this technique. After staining AY-27 cells with Rh123, mitochondrial potential was assessed by flow cytometry. Such as The highest kill in cells AY-27 rate was 44.56% at an average C3G concentration of 25 µg/ml.

Cyanidin-3-glucoside induces secretion of p53

Flow cytometry results shown in Figure 7 revealed a maximum killing rate of 44.56% for AY-27 cancer cells at an average C3G concentration of 25 µg/ml, as shown in Figures 5 and 6. C3G-treated cells exhibited a significant rightward shift in *p53*, an apoptotic marker.

Molecular Docking for Rat Bladder Cancer Cell Line

Table 2 and Figure 8 present the outcomes of the molecular docking approach of (Cyanidin 3-glucoside) (PDB ID: 5IRZ) Receptor. The molecular docking results indicate that Cyanidin 3-glucoside exhibited a stable and well-defined interaction, demonstrating the active region of the rat bladder cancer drug receptor, exhibiting a total binding power of −7.4815 calories per molecule.

Discussion

These results suggest the potential for C3G to inhibit the harmful proliferation of AY-27 cancer cells, which can lead to pathological changes, including DNA fragmentation, and other detrimental effects in AY-27 cells. It also influences Fas and ICAM expression, reduces Bcl-2 levels, and activates caspases 10, 9, 8, 6, 4, 3, and 2 in the AY-27 cell line, resulting in apoptosis, cytotoxicity, and

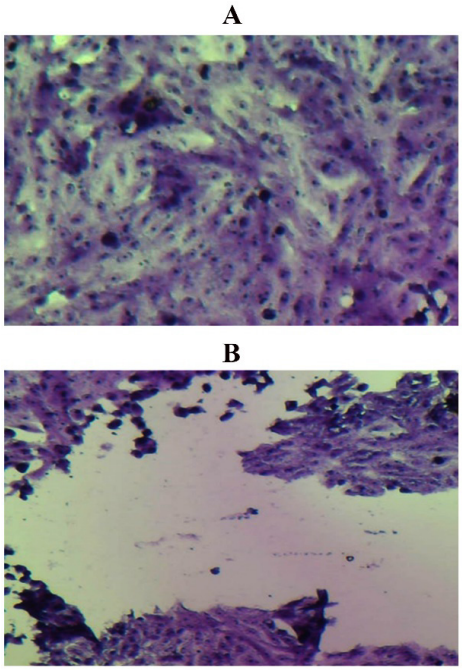

Figure 2. Morphological Changes in AY-27 Cells Following C3G Treatment. Magnification: 10x. A, Control untreated AY-27 cells. B, AY-27 cells after treatment with C3G at the IC_{50} concentration.

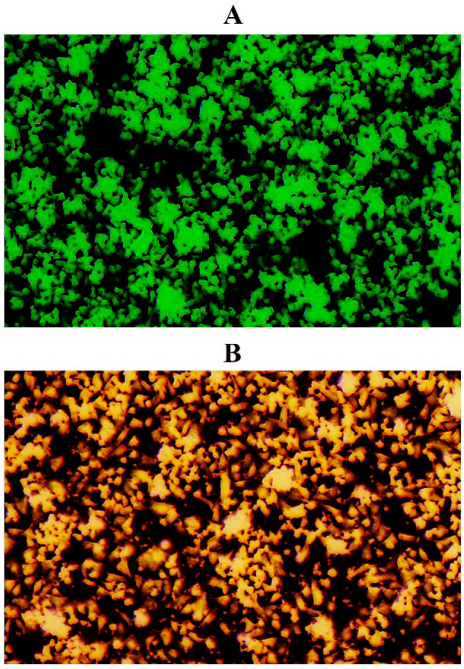

Figure 3. Apoptosis Markers in AY-27 Cells Following C3G Treatment. A, Control untreated AY-27 cells. B, AY-27 cells treated with C3G at the IC_{50} concentration

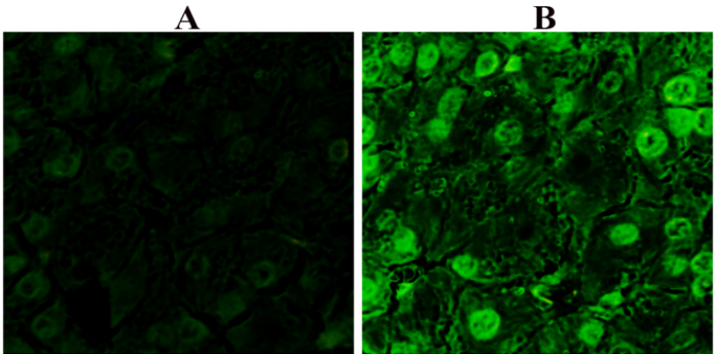

Figure 4. C3G Induces ROS Production in AY-27 Cells. A, Control AY-27 cells that are untreated. B, AY-27 cells treated with C3G at the IC_{50} concentration.

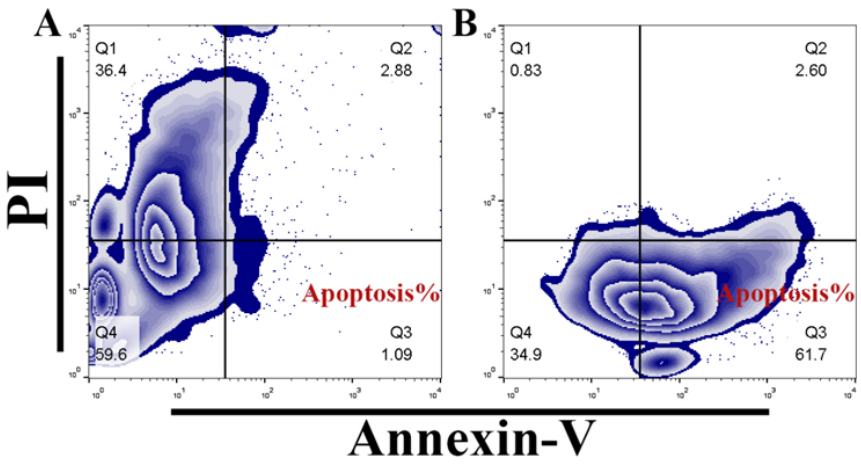

Figure 5. C3G Induces Apoptosis in AY-27. A, Control untreated AY-27 cells. B, AY-27 cells after been treated with C3G. at concentration IC_{50}.

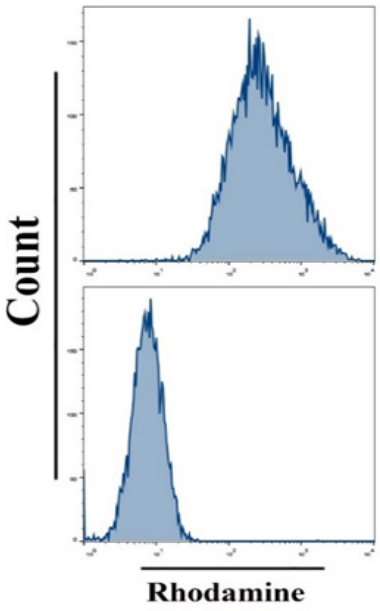

Figure 6. C3G Induces Mitochondrial Dysfunction in AY-27 Cells. Upper panel, control untreated AY-27 cells. Lower panel, AY-27 cells after being treated with C3G at the IC_{50} concentration.

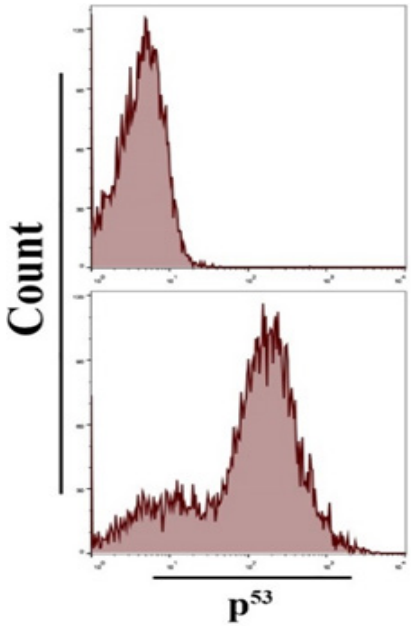

Figure 7. C3G Induces p53 Expression in AY-27 Cells. Upper panel: control untreated cells. Lower panel: AY-27 cells after being treated with C3G at the IC50 concentration.

cell death. This underscores the role of the C3G pigment in preventing and decreasing the risk of AY-27 rat and mouse cancers. Recent studies have shown a significant decrease in HeLa cell numbers following CPC treatment. Electron microscopy reveals CPC induces features of cytotoxicity and apoptosis, this includes swelling of the cell membrane, as well as loss of microvilli, shrinkage of cells, formation of dense cellular granules and condensation of chromatin. Additionally, research indicates that C3G boosts Fas protein expression as a pro-apoptotic factor and ICAM-1 as a cell adhesion molecule, while suppressing Bcl-2, which inhibits the mitochondria-dependent apoptosis pathway and regulates reactive oxygen species and cytochrome C release both key to apoptosis and growth regulation. These findings suggest that C3G can activate pro-apoptotic genes and downregulate anti-apoptotic genes, promoting tumor-induced apoptosis in BC cells in vitro [39, 40,41].

According to the findings presented in Figure 3 that using the double staining assay (AO/PI) as a fluorescent indicator allows one to detect any changes in the morphological shape of the nucleus of cancer cells, usually through the use of distinctive fluorescent colors. Following treatment with concentrations at half the IC50 of C3G, apoptotic cells increased dye permeability through the plasma membrane. Morphological changes were visualized using fluorescence microscopy, revealing membrane shrinkage, rupture, and gaps in lysosomes compared to untreated cells. The study findings suggest that C3G may serve as a therapeutic agent owing to its biological action, as it kills and inhibits cancer cell growth, repairs damaged cells, and prevents the migration and spread of nearby cells. This effect is concentration-dependent [42, 43]. Furthermore, is it possible that C3G

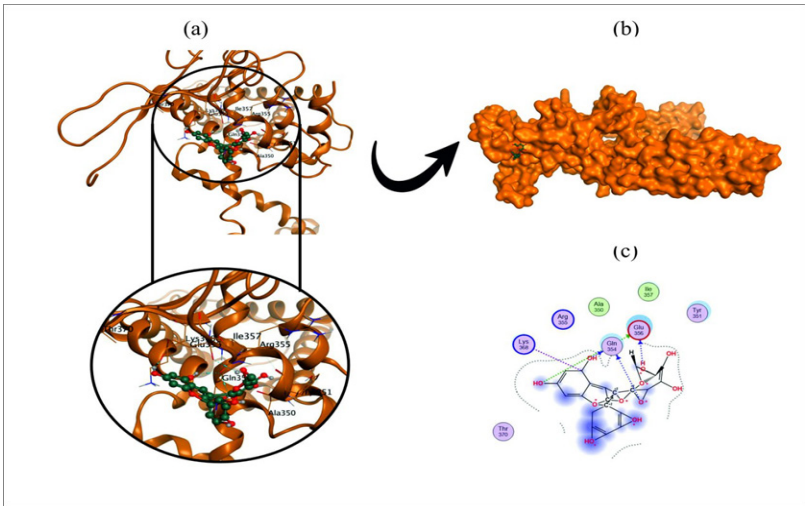

Figure 8. (a) Molecular docking of the ligand bond at the protein's active site. (b) Simulated molecular docking of cyanidin 3-glucoside with (PDB code: 5IRZ) the mouse bladder cancer receptor, a site representing the highest-ranking homologous binding. (c) Cyanidin 3-glucoside exhibits strong and stable binding to the mouse bladder cancer receptor, primarily through interactions with GLU356(D) and LYS368(D), a three-dimensional representation of all the amino acids surrounding the interacting homolog and the most stable. These results suggest its potential use as a natural inhibitor for bladder cancer treatment.

Table 2. Molecular Docking Results of (Cyanidin 3-glucoside) Ligand with the (Rat Bladder Cancer Cell Line) Receptor

			Bonds between Cyanidin 3-glucoside and the remains of the active site						
Compd. NO	Score (kcal/mol)	RMSD (Å)	Compd. Atoms	Receptor Atoms	Receptor Residues	Interaction	d (Å)	E (kcal/mol)	Total E (kcal/mol)
			O 21	OE1	GLU 356 (D)	H-donor	2.62	-2.7	
	-7.4815	2.139	O 23	O	GLU 356 (D)	H-donor	2.48	-1.5	-35.089
Rat Bladder			O 36	O	GLU 356 (D)	H-donor	2.67	-1.5	
			O 39	O	GLU 356 (D)	H-donor	2.76	-2	
			C 4	NZ	LYS 368 (D)	Ionic	3	-0.6	

can significantly halt the cancer cell cycle in the G0/G1 pathway, thereby inducing apoptosis and reducing the cancer cell's ability to invade neighboring cells by stimulating the Bax, PARP, and caspase-3 pathways [44-46].

To better understand the cytotoxic effects of C3G on the highly aggressive AY-27 cell line, We examined several indicators of cellular stress, such as ROS production, after exposure to an IC_{50} concentration (25.08 µg/ml) of the bio-compound C3G for 72 hours. ROS levels were notably higher in C3G-treated AY-27 cells, as detected by staining with 2′,7′-DCFH-DA. This dye acts as a general indicator of intracellular ROS; once inside the cell, esterases deacetylate it to form non-fluorescent DCFH, which ROS then oxidizes into the fluorescent compound 2′,7′-dichlorofluorescein (DCF). The DCF compound glows green at a wavelength of 485 nm as an excitation wave and at a wavelength of 530 nm as an emission wave. This study's results indicated that the toxic effect of the C3G compound in AY-27 cells was attributable to the overproduction of ROS, hence corroborating prior research findings. Oxidative stress impairs cellular homeostasis and destroys vital macromolecules, including lipids, nucleic acids, and proteins, resulting in programmed cell death (apoptosis). This study sought to assess the therapeutic efficacy of the natural chemical C3G on AY-27 cells by investigating its production of reactive oxygen species and its ability to induce apoptosis in cancer cells, and as shown in Figure 4. Overall, the data indicate that C3G induces apoptosis in AY-27 cells, depending on the dose and duration of exposure, primarily through excessive ROS production. Flow cytometry analysis revealed that treating pancreatic cancer AY-27 cells with C3G at their IC_{50} dose (25.08 µg/mL) significantly enhanced apoptosis. As indicated in Figure 5, there was a statistically significant increase in the percentage of dead cells 24 hours after treatment, this strong toxic effect of the compound on tumor cells was confirmed and established, by comparison with the untreated control group.

Matrix metalloproteases (MMPs) are key biomarkers and potential targets for cancer therapy. This is because any disruption to the mitochondrial pathway is a major factor in programmed cell death (apoptosis), and apoptosis is initiated through the mitochondrial pathway, which actively contributes to its activation by various stimuli. Deprivation of Δψm and release of cyst-c into the cell cytoplasm are among the most important changes associated with programmed cell death in mitochondria, leading to activation of cas-3 proteins via cas-9. We assessed the rate of apoptosis in AY-27 cells

followingexposed to C3G for 24 hours exhibited reduced Rh123 staining, indicatingllustrated in Figure 6. Cells subjected to C3G for 24 hours exhibited diminished Rh123 staining, signifying a decreased mitochondrial potential relative to untreated cells [47]. The highest kill rate was 44.56% in AY-27 cells at an average C3G concentration of 25 µg/ml [46]. It has been shown that Bcl-2 proteins have a carboxyl terminal region where this region targets the outer membrane of the mitochondria as well as its nuclear envelope by binding to its terminal group. translocating to mitochondria, and triggering apoptosis. Once activated, these proteins can bind to other anti-apoptotic proteins, preventing their function and indorsing cell death in bladder tumor cells [42, 48].

Apoptosomes can be observed in programmed cell death events in tumor cells, leading to the orderly disintegration of cancerous cells [49]. In this study, in Figure 7, we measured *p53* expression levels. The results indicated that treating AY-27 cells with C3G caused an increase in the *p53* pathway, compared to the results in the control group. *P53* functions as a cellular stress sensor and as part of a signal transduction pathway that induces cell cycle arrest following DNA damage. Additionally, the extrinsic and intrinsic death pathways can induce programmed cell death by upregulating the cas-8 and *p53* pathways [39, 50]. Previous testing clearly demonstrated that C3G can induce mitochondria-dependent apoptosis. For cell death to occur, there are two important pathways: the extrinsic pathway (mediated by programmed cell death receptors) and the intrinsic pathway (regulated at the level of mitochondrial proteins or receptors). The extrinsic pathway is triggered by signals from the outer surface the purines of cancer cells, specifically Fas/FasL, which draw in the associated with Fas death domain (FADD). The FADD-Fas complex pathway can induce procaspase-8. This dynamic and bioactive complex, commonly known as the DISC (Dissociative Cell Death Signaling Complex), is capable of activating casp-3, important to cell death. The activity of the *p53* protein has been investigated using flow cytometry [20, 50-52].

This relatively low binding score reflects a strong affinity and good fitting of the ligand within the receptor's active pocket are shown in Table 2 and Figure 8. Several hydrogen bonds were observed between the oxygen atoms of the ligand (O21, O23, O36, O39, and C4) and the receptor residues, mainly GLU356(D) and LYS368(D) [53, 54]. The interactions included multiple H-donor bonds and one ionic interaction, with bond distances ranging from 2.48 to 3.00 Å, which are within the optimal range for hydrogen bonding. The repeated interactions with GLU356(D) These remnants demonstrate their important role within the active site by fixing the link. Moreover, the ionic interaction with LYS368(D) enhances the electrostatic attraction, thereby increasing the overall stability of the complex. Energetically, the partial interaction energies (ranging from −2.7 to −0.6 kcal/mol) contribute additively to a highly negative total binding energy, indicating a strong and stable complex formation between the ligand and the receptor. Overall, these findings suggest that Cyanidin 3-glucoside has a notable binding potential toward the rat bladder cancer receptor, highlighting its possible role as an effective inhibitory compound capable of interfering with crucial active-site residues [55, 56].

In conclusion, the present study sought to investigate an alternate approach to mitigate bladder cancer incidence in mice, emphasizing natural, environmentally sustainable substances instead of traditional chemical therapies. The study specifically examined flavonoids originating from marine algae, focusing on anthocyanins such as cyanidin-3-glucoside (C3G), a natural pigment in vitro, C3G demonstrated efficacy in inhibiting or eradicating cancer cells (CC), as well as in vivo, including the AY-27 bladder cancer strain in mice. The study investigated the influence of C3G on bladder cancer growth in isolated cells and its ability to induce multiple cellular pathways, including cytotoxicity, apoptosis, the *p53* pathway, the mitochondrial pathway, and microenvironmental fusion. The most pronounced cytotoxic effect was observed at a C3G dose of 100 µg/ml, resulting in a cell death rate of 84.43%. The minimal cytotoxic impact recorded was 9.45% at a dose of 6.25 µg/ml. Apoptosis was assessed via DNA damage, while analysis of the mitochondrial pathway indicated that C3G caused mitochondrial dysfunction in AY-27 cells, resulting in a loss of membrane potential relative to untreated cells. C3G was also experiential to enhance *p53* gene expression, hence reinforcing its function in tumor suppression. These data indicate that C3G effectively induces apoptosis, consequently suppressing the growth and advancement of the AY-27 bladder cancer cell line. Therefore, the C3G compound shows promising therapeutic potential as a drug for bladder cancer in mice. Cyanidin 3-glucoside binding was mimicked with a mouse bladder cancer cell line. These interactions indicate a significant inhibitory effect against bladder cancer targets.

Author Contribution Statement

H. A. A, A. H. A., E.A.A. , S. A. J. T. H. A. and M. S. J. conceptualized the study and drafted the manuscript. H. A. A, A. H. A., and E.A.A. responsible for running experiments, while H. A. A, A. H. A., and E.A.A. collected the data. H. A. A, A. H. A., E.A.A. , S. A. J. T. H. A. and M. S. J. were responsible for data extraction and analysis. All authors read and approved the final manuscript.

Acknowledgements

The authors appreciated University of technology- Iraq for supporting this study.

Data Availability

All data generated during this study are included in this article

References

1. Abdelaal Ns, El Seedy Gm, Elhassaneen Ya. Chemical composition, nutritional value, bioactive compounds content and biological activities of the brown alga (sargassum subrepandum) collected from the mediterranean sea, egypt.

Alexandria science exchange journal. 2021;42(4):893-906.
2. Song Y, Liu X, Cheng W, Li H, Zhang D. The global, regional and national burden of stomach cancer and its attributable risk factors from 1990 to 2019. Sci Rep. 2022;12(1):11542. https://doi.org/10.1038/s41598-022-15839-7.
3. Ghufran MS, Soni P, Duddukuri GR. The global concern for cancer emergence and its prevention: A systematic unveiling of the present scenario. In: Arunachalam K, Yang X, Puthanpura Sasidharan S, editors. Bioprospecting of tropical medicinal plants. Cham: Springer Nature Switzerland; 2023. p. 1429-55.
4. van den Boogaard WMC, Komninos DSJ, Vermeij WP. Chemotherapy side-effects: Not all DNA damage is equal. Cancers (Basel). 2022;14(3). https://doi.org/10.3390/cancers14030627.
5. Anand R, Mohan L, Bharadvaja N. Disease prevention and treatment using β-carotene: The ultimate provitamin a. Rev Bras Farmacogn. 2022;32(4):491-501. https://doi.org/10.1007/s43450-022-00262-w.
6. Pradhan B, Ki JS. Antioxidant and chemotherapeutic efficacies of seaweed-derived phlorotannins in cancer treatment: A review regarding novel anticancer drugs. Phytotherapy Research. 2023 May;37(5):2067-91.
7. Matin M, Koszarska M, Atanasov AG, Król-Szmajda K, Jóźwik A, Stelmasiak A, et al. Bioactive potential of algae and algae-derived compounds: Focus on anti-inflammatory, antimicrobial, and antioxidant effects. Molecules. 2024;29(19). https://doi.org/10.3390/molecules29194695.
8. Barsanti L, Gualtieri P. Glucans, paramylon and other algae bioactive molecules. Int J Mol Sci. 2023;24(6). https://doi.org/10.3390/ijms24065844.
9. Shirolkar A, Chougule S, Ranade A, Pawase A, Gaidhani S, Pawar S. The potential applications of plant-based anti-cancer compounds and their chemical derivatives. Int J Pharm Sci Res. 2022;13:4794-804. https://doi.org/10.13040/IJPSR.0975-8232.13(12).4794-04.
10. Amstutz rp, dufour p. Colchicine in cancer therapy: 50 years of promise. Curr oncol rep. 2019;21(5):43.
11. Sulasmi E, Wuriana Z, Sari R, Rohmawati U. Flavonoid characterization in ferns from baluran national park. IOP Conference Series: Earth and Environmental Science. 2019;276:012033. https://doi.org/10.1088/1755-1315/276/1/012033.
12. Li J, Guo Y, Ma L, Liu Y, Zou C, Kuang H, et al. Synergistic effects of alginate oligosaccharide and cyanidin-3-o-glucoside on the amelioration of intestinal barrier function in mice. Food Science and Human Wellness. 2023;12(6):2276-85. https://doi.org/10.1016/j.fshw.2023.03.047.
13. Chen J, Xu B, Sun J, Jiang X, Bai W. Anthocyanin supplement as a dietary strategy in cancer prevention and management: A comprehensive review. Crit Rev Food Sci Nutr. 2022;62(26):7242-54. https://doi.org/10.1080/10408398.2021.1913092.
14. Grosso G, Godos J, Lamuela-Raventos R, Ray S, Micek A, Pajak A, et al. A comprehensive meta-analysis on dietary flavonoid and lignan intake and cancer risk: Level of evidence and limitations. Mol Nutr Food Res. 2017;61(4). https://doi.org/10.1002/mnfr.201600930.
15. Lin BW, Gong CC, Song HF, Cui YY. Effects of anthocyanins on the prevention and treatment of cancer. Br J Pharmacol. 2017;174(11):1226-43. https://doi.org/10.1111/bph.13627.
16. Gérard V, Ay E, Morlet-Savary F, Graff B, Galopin C, Ogren T, et al. Thermal and photochemical stability of anthocyanins from black carrot, grape juice, and purple sweet potato in model beverages in the presence of ascorbic acid. J Agric Food Chem. 2019;67(19):5647-60. https://doi.org/10.1021/acs.jafc.9b01672.
17. Khoo HE, Azlan A, Tang ST, Lim SM. Anthocyanidins and anthocyanins: Colored pigments as food, pharmaceutical ingredients, and the potential health benefits. Food Nutr Res. 2017;61(1):1361779. https://doi.org/10.1080/16546628.2017.1361779.
18. Trouillas P, Sancho-García JC, De Freitas V, Gierschner J, Otyepka M, Dangles O. Stabilizing and modulating color by copigmentation: Insights from theory and experiment. Chem Rev. 2016;116(9):4937-82. https://doi.org/10.1021/acs.chemrev.5b00507.
19. Kowalczyk T, Muskała M, Merecz-Sadowska A, Sikora J, Picot L, Sitarek P. Anti-inflammatory and anticancer effects of anthocyanins in in vitro and in vivo studies. Antioxidants (Basel). 2024;13(9). https://doi.org/10.3390/antiox13091143.
20. Kareem haider a, alghanmi h. Effects of various light intensities on phycocyanin composition of cyanobacterium limnospira fusiformis (voronichin) nowicka-krawczyk, mühlsteinová & hauer. Malays j sci. 2023;1-6. https://doi.Org/10.22452/mjs.Vol42no1.1.
21. Wang LS, Stoner GD. Anthocyanins and their role in cancer prevention. Cancer Lett. 2008;269(2):281-90. https://doi.org/10.1016/j.canlet.2008.05.020.
22. Andersen OM, Markham KR. Flavonoids: Chemistry, biochemistry and applications. Crc press; 2005 dec 9.
23. Boulton r. The copigmentation of anthocyanins and its role in the color of red wine: A critical review. Am j enol vitic. 2001:2001;52:67-87. https://doi.org/10.5344/ajev.2001.52.2.67.
24. Garcia C, Blesso CN. Antioxidant properties of anthocyanins and their mechanism of action in atherosclerosis. Free Radic Biol Med. 2021;172:152-66. https://doi.org/10.1016/j.freeradbiomed.2021.05.040.
25. Kamiloglu S, Günal-Köroğlu D, Ozdal T, Tomas M, Capanoglu E. Recent advances on anti-diabetic potential of pigmented phytochemicals in foods and medicinal plants. Phytochemistry Reviews. 2025;24(3):2203-33. https://doi.org/10.1007/s11101-024-10014-4.
26. Francis AP, Ahmad A, Nagarajan SD, Yogeeswarakannan HS, Sekar K, Khan SA, Meenakshi DU, Husain A, Bazuhair MA, Selvasudha N. Development of a novel red clay-based drug delivery carrier to improve the therapeutic efficacy of acyclovir in the treatment of skin cancer. Pharmaceutics. 2023 Jul 10;15(7):1919.
27. Levardon H, Yonker LM, Hurley BP, Mou H. Expansion of airway basal cells and generation of polarized epithelium. Bio Protoc. 2018;8(11). https://doi.org/10.21769/BioProtoc.2877.
28. Tunç T. Synthesis and characterization of silver nanoparticles loaded with carboplatin as a potential antimicrobial and cancer therapy. Cancer Nanotechnol. 2024;15(1):2. https://doi.org/10.1186/s12645-023-00243-1.
29. Alharbi NS, Alsubhi NS. Green synthesis and anticancer activity of silver nanoparticles prepared using fruit extract of azadirachta indica. J Radiat Res Appl Sci. 2022;15(3):335-45. https://doi.org/10.1016/j.jrras.2022.08.009.
30. Kumar G, Virmani T, Sharma A, Pathak K. Codelivery of phytochemicals with conventional anticancer drugs in form of nanocarriers. Pharmaceutics. 2023;15(3). https://doi.org/10.3390/pharmaceutics15030889.
31. Noori SD, Kadhi MS, Najm MAA, Oudah KH, Qasim QA, Al-Salman HNK. In-vitro evaluation of anticancer activity of natural flavonoids, apigenin and hesperidin. Materials Today: Proceedings. 2022;60:1840-3. https://doi.org/https://doi.org/10.1016/j.matpr.2021.12.506.
32. Beheshti F, Shabani AA, Akbari Eidgahi MR, Kookhaei P, Vazirian M, Safavi M. Anticancer activity of ipomoea

purpurea leaves extracts in monolayer and three-dimensional cell culture. Evid Based Complement Alternat Med. 2021;2021:6666567. https://doi.org/10.1155/2021/6666567.
33. Mohammed SAA, Khashan KS, Jabir MS, Abdulameer FA, Sulaiman GM, Al-Omar MS, et al. Copper oxide nanoparticle-decorated carbon nanoparticle composite colloidal preparation through laser ablation for antimicrobial and antiproliferative actions against breast cancer cell line, mcf-7. Biomed Res Int. 2022;2022:9863616. https://doi.org/10.1155/2022/9863616.
34. Liu M, Kinghorn AB, Wang L, Bhuyan SK, Shiu SC, Tanner JA. The evolution and application of a novel DNA aptamer targeting bone morphogenetic protein 2 for bone regeneration. Molecules. 2024;29(6). https://doi.org/10.3390/molecules29061243.
35. Yazdanyar A, Cai CL, Aranda JV, Shrier E, Beharry KD. Comparison of bevacizumab and aflibercept for suppression of angiogenesis in human retinal microvascular endothelial cells. Pharmaceuticals (Basel). 2023;16(7). https://doi.org/10.3390/ph16070939.
36. Chelliah R, Oh DH. Screening for anticancer activity: dual staining method. InMethods in Actinobacteriology 2022 Jan 1 (pp. 427-429). New York, NY: Springer US.
37. Brown AM. A new software for carrying out one-way anova post hoc tests. Comput Methods Programs Biomed. 2005;79(1):89-95. https://doi.org/10.1016/j.cmpb.2005.02.007.
38. Afifah S, Mudzakir A, Nandiyanto ABD. How to calculate paired sample t-test using spss software: From step-by-step processing for users to the practical examples in the analysis of the effect of application anti-fire bamboo teaching materials on student learning outcomes. Indonesian journal of teaching in science. 2022;2(1):81-92. https://doi.org/10.17509/ijotis.V2i1.45895
39. Xuan L, Hu JH, Bi R, Liu SQ, Wang CX. Andrographolide inhibits proliferation and promotes apoptosis in bladder cancer cells by interfering with nf- κ b and pi3k/akt signaling in vitro and in vivo. Chin J Integr Med. 2022;28(4):349-56. https://doi.org/10.1007/s11655-022-3464-4.
40. van Eyk AD. The effect of five artificial sweeteners on caco-2, ht-29 and hek-293 cells. Drug Chem Toxicol. 2015;38(3):318-27. https://doi.org/10.3109/01480545.2014.966381.
41. Li B, Zhang X, Gao M, Chu X. Study of regulatory effect of phycocyanin on cd59 gene expression of hela cells. 2006;16:196-200.
42. Lv Y, Liu Z, Jia H, Xiu Y, Liu Z, Deng L. Properties of flavonoids in the treatment of bladder cancer. Experimental and Therapeutic Medicine. 2022 Sep 19;24(5):676.
43. Ansary j. Evaluation of the anti-proliferative effect of phenolic compounds from garlic on human breast cancer cells through the modulation of different molecular mechanisms involved in their growth and proliferation; 2022.
44. Mottaghipisheh J, Doustimotlagh AH, Irajie C, Tanideh N, Barzegar A, Iraji A. The promising therapeutic and preventive properties of anthocyanidins/anthocyanins on prostate cancer. Cells. 2022;11(7). https://doi.org/10.3390/cells11071070.
45. Xia Y, Chen R, Lu G, Li C, Lian S, Kang TW, et al. Natural phytochemicals in bladder cancer prevention and therapy. Front Oncol. 2021;11:652033. https://doi.org/10.3389/fonc.2021.652033.
46. Adachi M, Imai K. The proapoptotic BH3-only protein BAD transduces cell death signals independently of its interaction with Bcl-2. Cell Death & Differentiation. 2002 Nov;9(11):1240-7.
47. Saini MK, Sanyal SN, Vaiphei K. Piroxicam and c-phycocyanin mediated apoptosis in 1,2-dimethylhydrazine dihydrochloride induced colon carcinogenesis: Exploring the mitochondrial pathway. Nutr Cancer. 2012;64(3):409-18. https://doi.org/10.1080/01635581.2012.655402.
48. Jabir MS, Saleh YM, Sulaiman GM, Yaseen NY, Sahib UI, Dewir YH, et al. Green synthesis of silver nanoparticles using annona muricata extract as an inducer of apoptosis in cancer cells and inhibitor for nlrp3 inflammasome via enhanced autophagy. Nanomaterials (Basel). 2021;11(2). https://doi.org/10.3390/nano11020384.
49. Rahman KMM, Bist G, Kumbham S, Foster BA, Woo S, You Y. Mitochondrial targeting improves the selectivity of singlet-oxygen cleavable prodrugs in nmibc treatment. Photochem Photobiol. 2024;100(6):1622-35. https://doi.org/10.1111/php.13928.
50. Luo Y, Fu X, Ru R, Han B, Zhang F, Yuan L, et al. Cpg oligodeoxynucleotides induces apoptosis of human bladder cancer cells via caspase-3-bax/bcl-2-*p53* axis. Arch Med Res. 2020;51(3):233-44. https://doi.org/10.1016/j.arcmed.2020.02.005.
51. Al-obaidy ha, leelo ak. Detection of bioactive compound from microscopic blue-green algae gloeocapsopsis crepidinum under the effect of different light intensities. International journal of research and innovation in applied science. 2025;10(5):130-41. . https://doi.org/10.51584/IJRIAS.2025.100500012.
52. Al-obaidy, haider ammar kareem leelo. Effect of light intimities and nutrients on phycocyanin production from some algal species and testing its biological activity on cancer cells. College of education-university al-qadisiyah-plant science; 2022.
53. Ibraheem hh, shubrem as, al-majedy yk, issa aa. Experimental studies on the corrosion inhibition performance of chalcone derivative for mild steel in acid and alkaline solution. Inaip conference proceedings 2022 jul 11 (vol. 2443, no. 1, p. 030044). Aip publishing llc.
54. Chemical computing group ulc, molecular operating environment (moe), version 2024.06, montreal, qc, canada: Chemical computing group, 2024.
55. Al-majedy yk, ibraheem hh, issa aa. Antioxidant, antimicrobial activity and quantum chemical studies of 4-methyl-7-hyroxy coumarin derivatives. In1st diyala international conference for pure and applied science: Icpas2021 2023 may 22 (vol. 2593, no. 1, p. 060002). Aip publishing llc.
56. Alkhafaji AA, Ahmed HM, Queen BK, Issa AA, Sulaiman GM, Elkashef AA, et al. Recent perspective on polymeric semimetal (si, ge and as) and nonmetal (n and p) doped c70-fullerene system: Comparative electronic, dynamic behavior and chemotherapy docking with admet analysis. Journal of Organometallic Chemistry. 2024;1022:123417. https://doi.org/10.1016/j.jorganchem.2024.123417.